ARTICLE

Supplementary Information (SI) for: Persistence of Ce^{3+} Species on the Surface of Ceria during Redox Cycling: A Modulated Chemical Excitation Investigation

C. Hachemi[a], H. Dib[b], M. Debbichi[c], M. Badawi[d], C. Eads[e], M. Ibrahim[b], S. Loridant[a], J.Knudsen[e], H. Kaper[b], L. Cardenas[a*]

a. Univ. Lyon, Université Claude Bernard-Lyon 1, CNRS, IRCELYON-UMR 5256, 2 av. A. Einstein, F-69626 Villeurbanne Cedex, France.

b. Saint Gobain Recherche Provence, 550, Ave Alphonse Jauffret, 84306 Cavaillon, France.

c. Université de Monastir, Faculté des Sciences de Monastir, Laboratoire de la matière condensée et nanosciences, LR11ES40, 5019 Monastir, Tunisia.

d. Université de Lorraine, CNRS, L2CM, F-54000 Nancy, France.

e. Division of Synchrotron Radiation Research, Department of Physics, Lund University, Lund, Sweden. MAX IV Laboratory, Lund University, Lund, Sweden.

Corresponding Author: *E-mail: luis.cardenas@ircelyon.univ-lyon1.fr

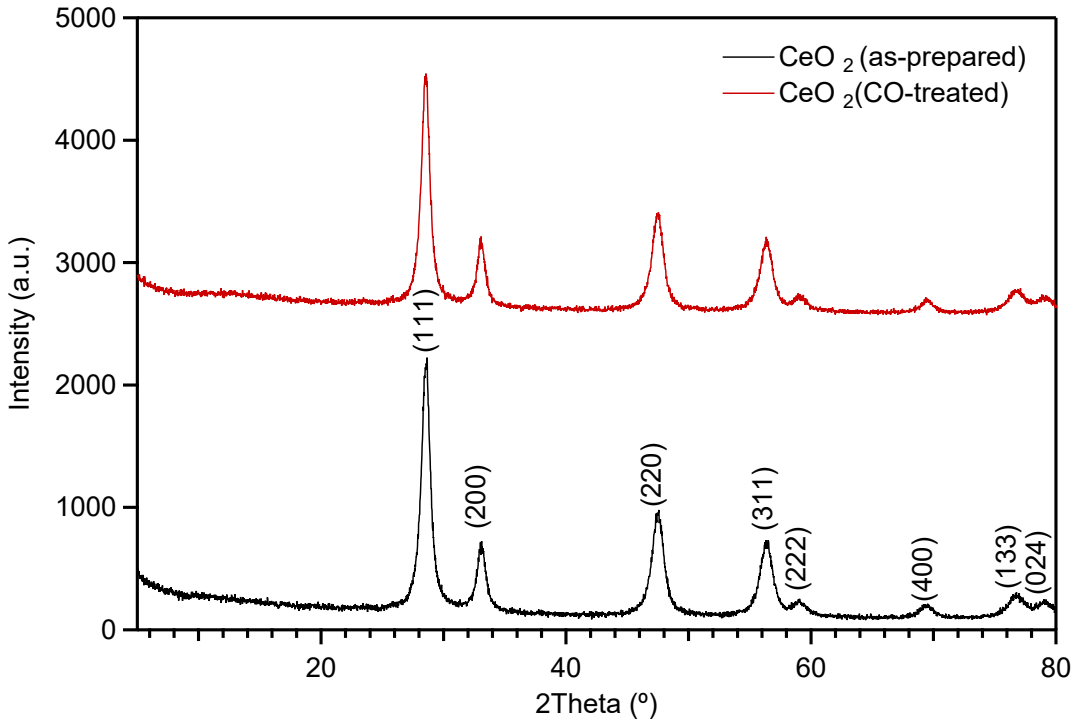

Figure S1: XRD patterns of the as-prepared ceria powder (black) and CO-treated ceria at 400 °C for 1 h (red). No apparent bulk lattice expansion was observed upon CO exposure, suggesting only surface modifications. The crystallites were estimated to be 9.9 nm and 10.3 nm for the as-prepared and CO-exposed ceria, respectively.

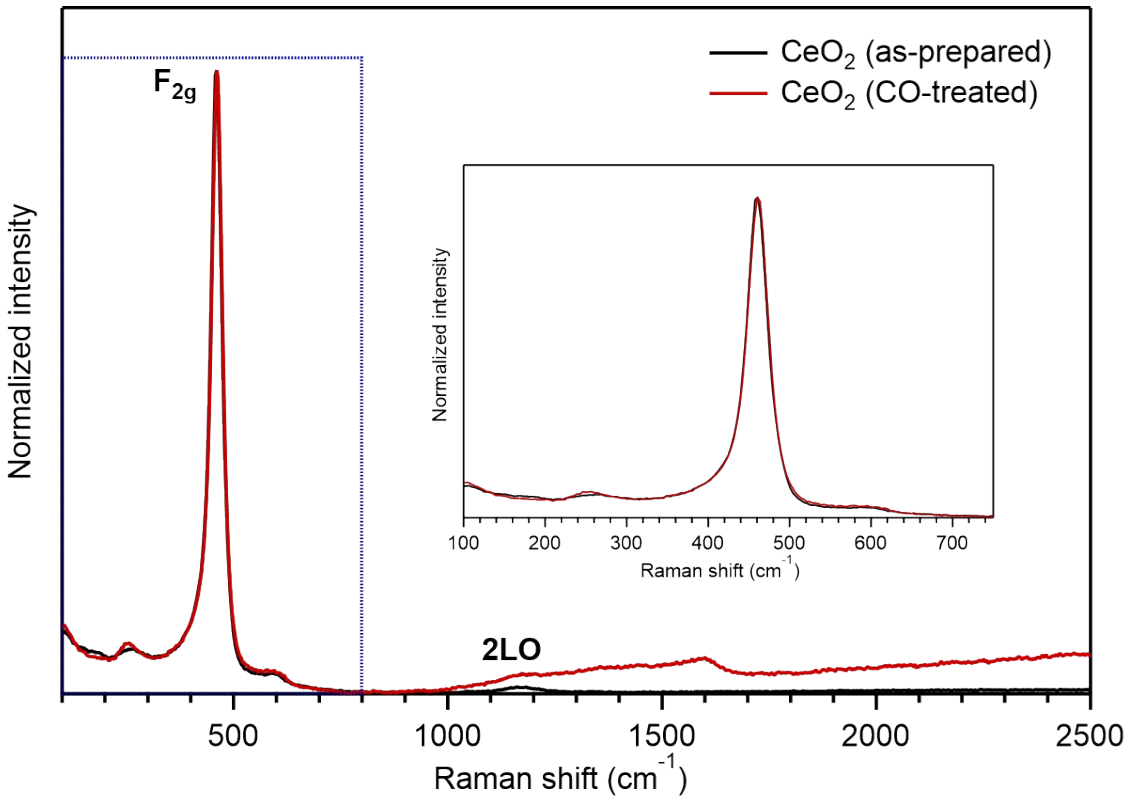

Figure S2: Raman spectra of the as-prepared ceria powder (black) and CO-treated Ceria at 400 °C for 1 h (red). No significant change of the F_{2g} vibrational mode was observed, but a novel band appeared at about 1600 cm^{-1} with a continuous fluorescence background. The apparent changes are likely due to the reduction of adsorbed surface carbon species before the CO reduction. Additionally, no Ce^{3+} electronic transition was observed at around 2100-2150 cm^{-1} ($^2F_{5/2} \rightarrow {}^2F_{7/2}$) for both samples[1].

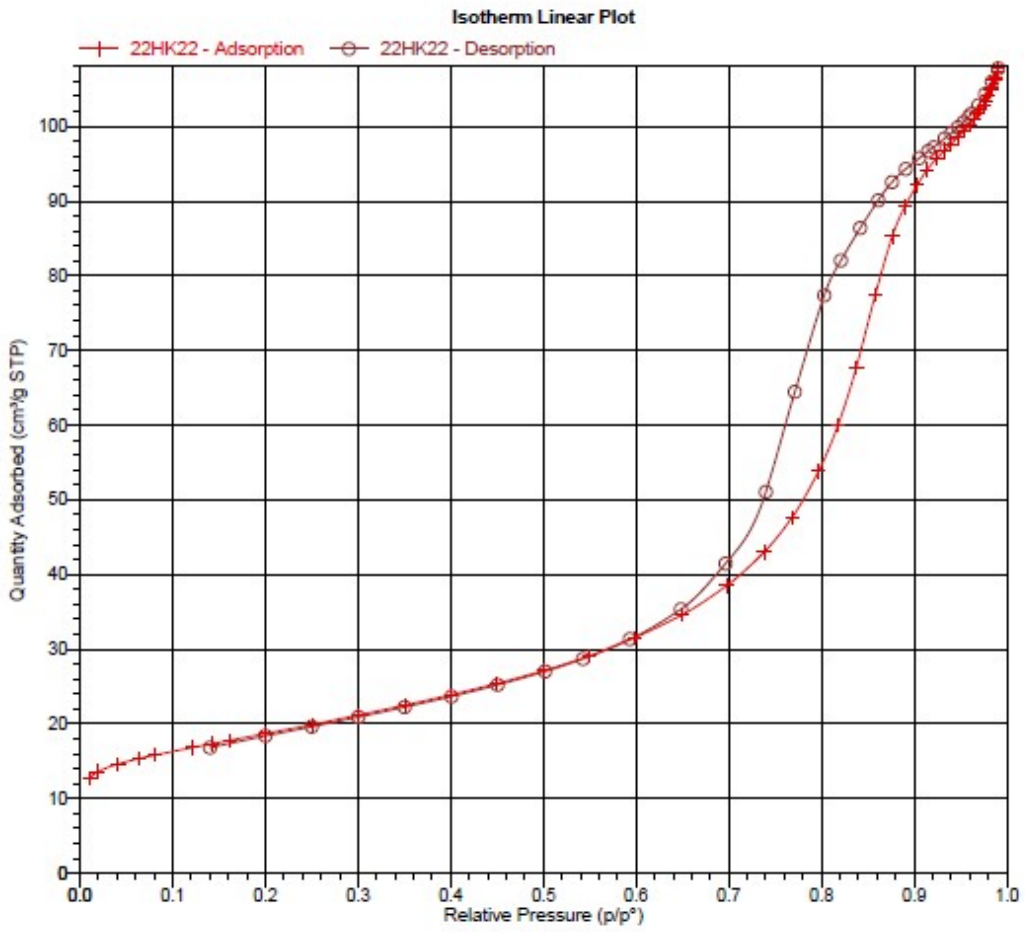

Figure S3: Nitrogen adsorption-desorption isotherms (measured at 77 K) of the as-prepared ceria powder. The sample showed a type IV isotherm with a BET surface area of 65.11 $m^2.g^{-1}$ (± 0.34 $m^2.g^{-1}$), and a pore volume of 0.15 $cm^3.g^{-1}$.

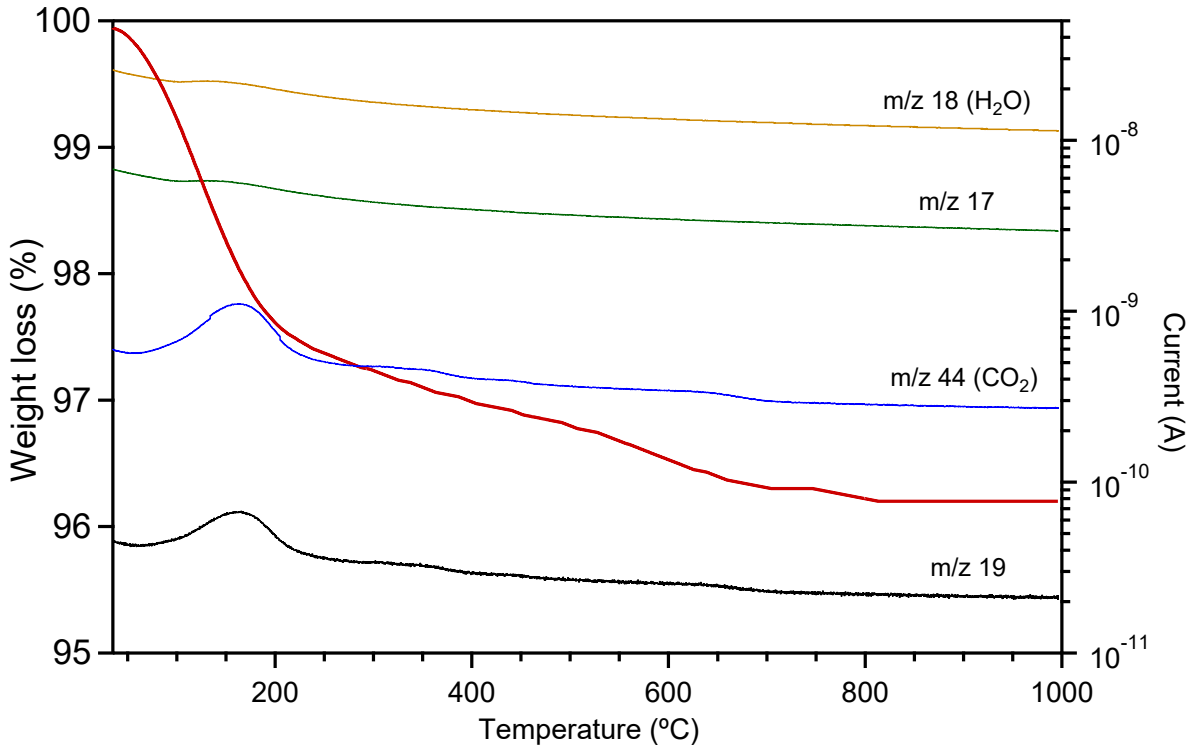

Figure S4: MS-TGA of the as-prepared Ceria performed under O_2 - A total mass loss of 3.8 % was observed and mainly attributed to the desorption of water and carbon dioxide.

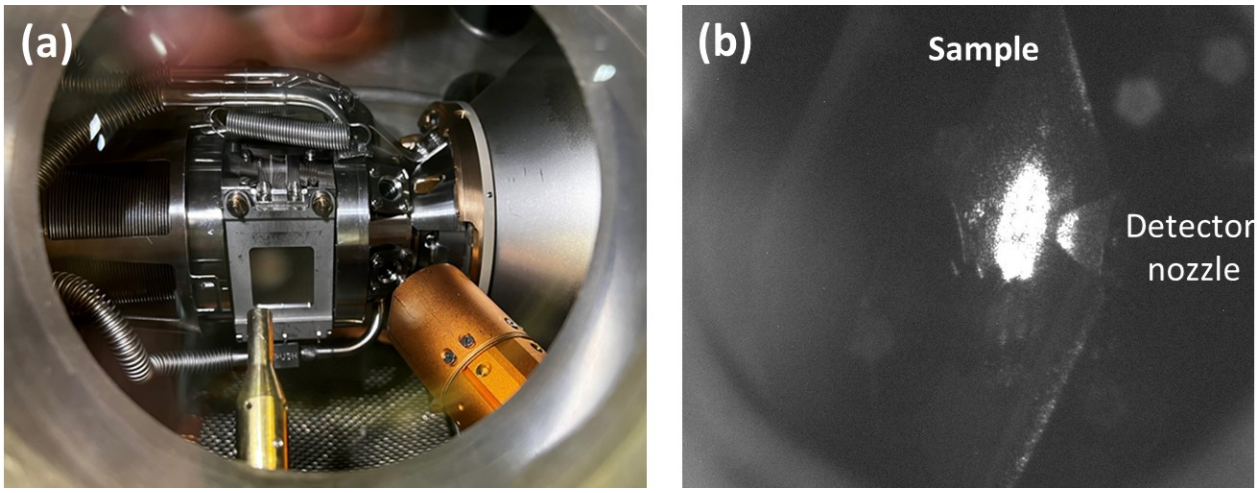

Figure S5: (a) Near Ambient Pressure Cell of the SPECIES endstation (volume ≈1L). (b) CeO_2 sample in analysis position.

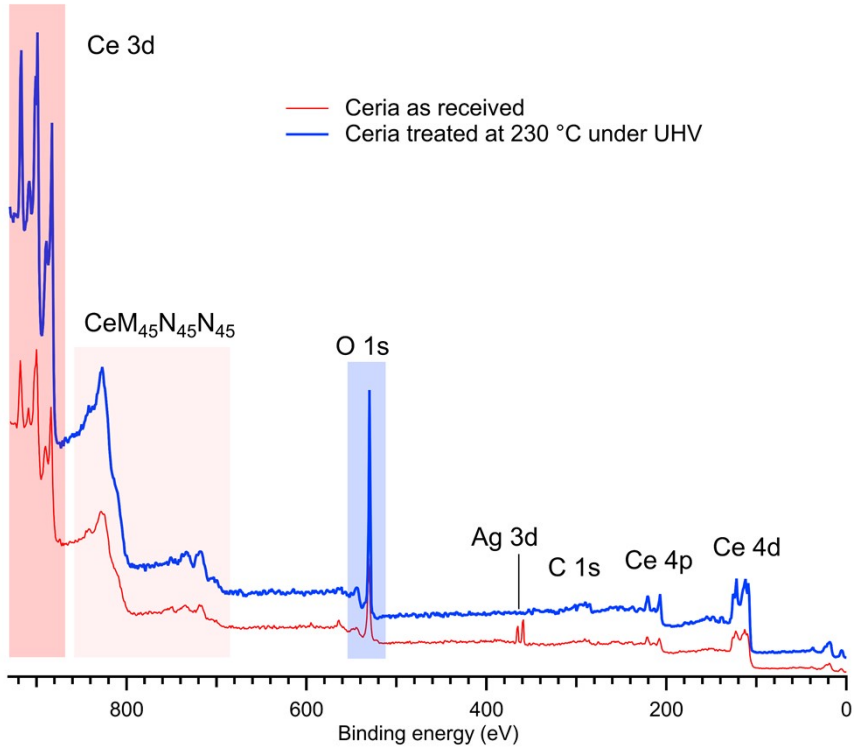

Figure S6: Survey spectra, acquired from the surface of CeO_2 as-received and treated at 230 °C under UHV conditions prior to Modulated Chemical Excitation RPES measurements, reveal Ce and O as the dominant species with minimal C contamination.

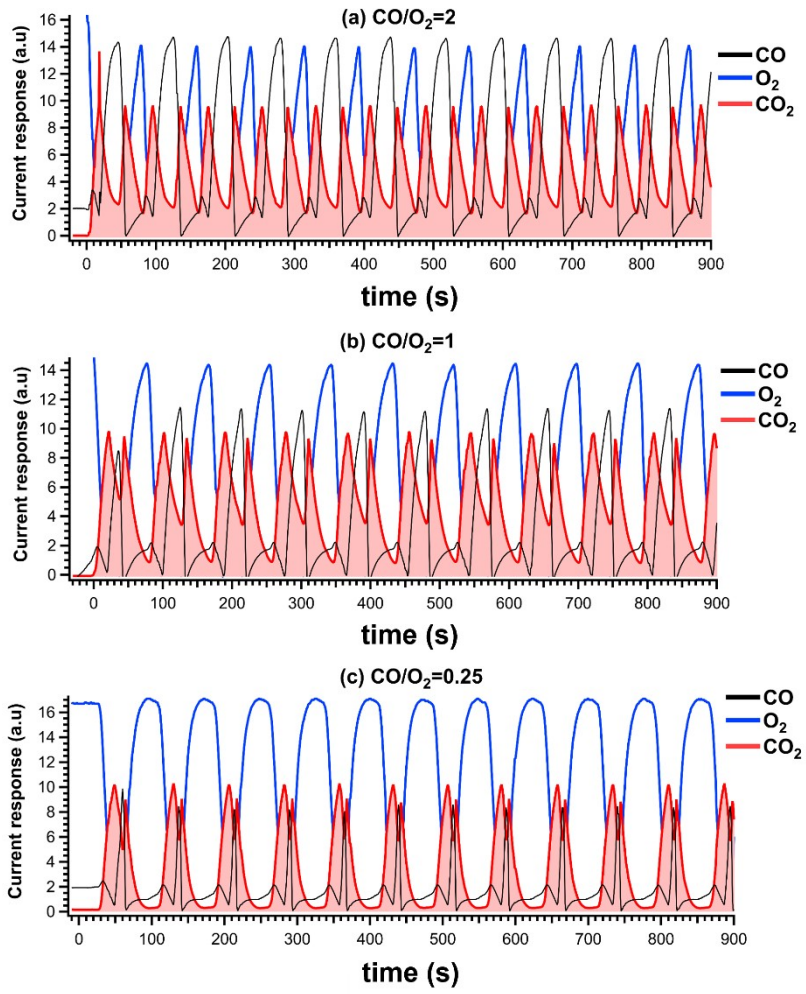

Figure S7: Transient mass spectra of CO (black), O_2 (blue), and CO_2 (red) obtained at 420 °C showing CO_2 production under the injection of CO/O_2 with a reactants ratio of 2(a), 1(b), and 0.25(c).

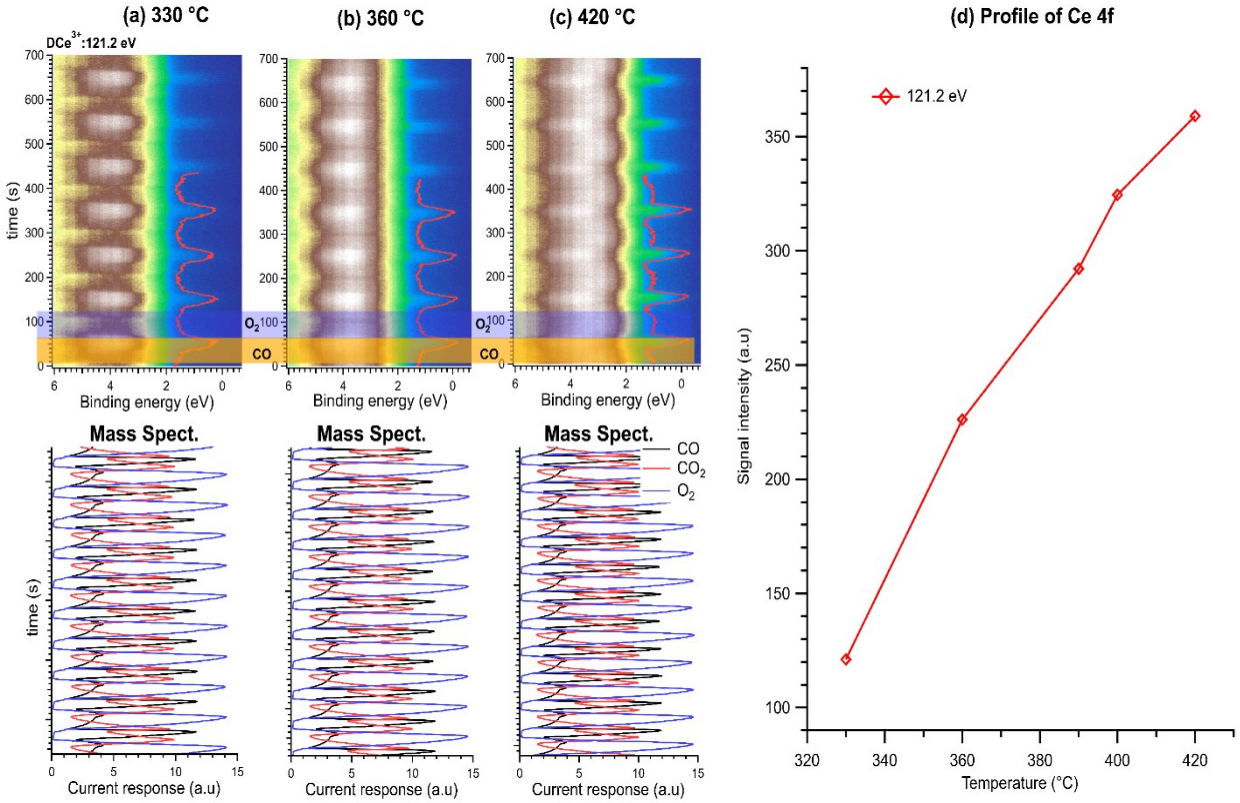
(a) 330 °C
(b) 360 °C
(c) 420 °C
(d) Profile of Ce 4f
DCe3+:121.2 eV
time (s)
Binding energy (eV)
O2
CO
Mass Spect.
CO
CO2
O2
Current response (a.u)
121.2 eV
Signal intensity (a.u)
Temperature (°C)

Figure S8: Modulated chemical excitation RPES spectra measured while CO (yellow band) and O_2 (blue band) are pulsed with a flow ratio CO:O_2 = 1. The experiments were performed while ceria is kept at (a) 330 °C, (b) 360 °C, and (c) 420 °C, respectively. The pulse duration of each reactant gas was 40 s. RPES were obtained at the threshold energy of 121.2 eV and Ce^{3+} excitation. Here, spectra were aligned to the mass spectrometry (MS) signal of CO (black). The synchronization between CO pulses and the Ce 4f event (red intensity profile) is established by the simultaneous alignment between the formation of the mass signal CO (m/z = 28) measured by the MS (bottom) and the detection of the Ce 4f in the valence band by RPES (red profile). Thus, after identifying Ce 4f as a reference event, we follow its formation and extinction during periodic CO and O_2 injection cycles, respectively. The red profile centered on the Ce 4f state at ≈ 1 eV reveals the increase of Ce^{3+} phase intensity as a function of temperature (d).

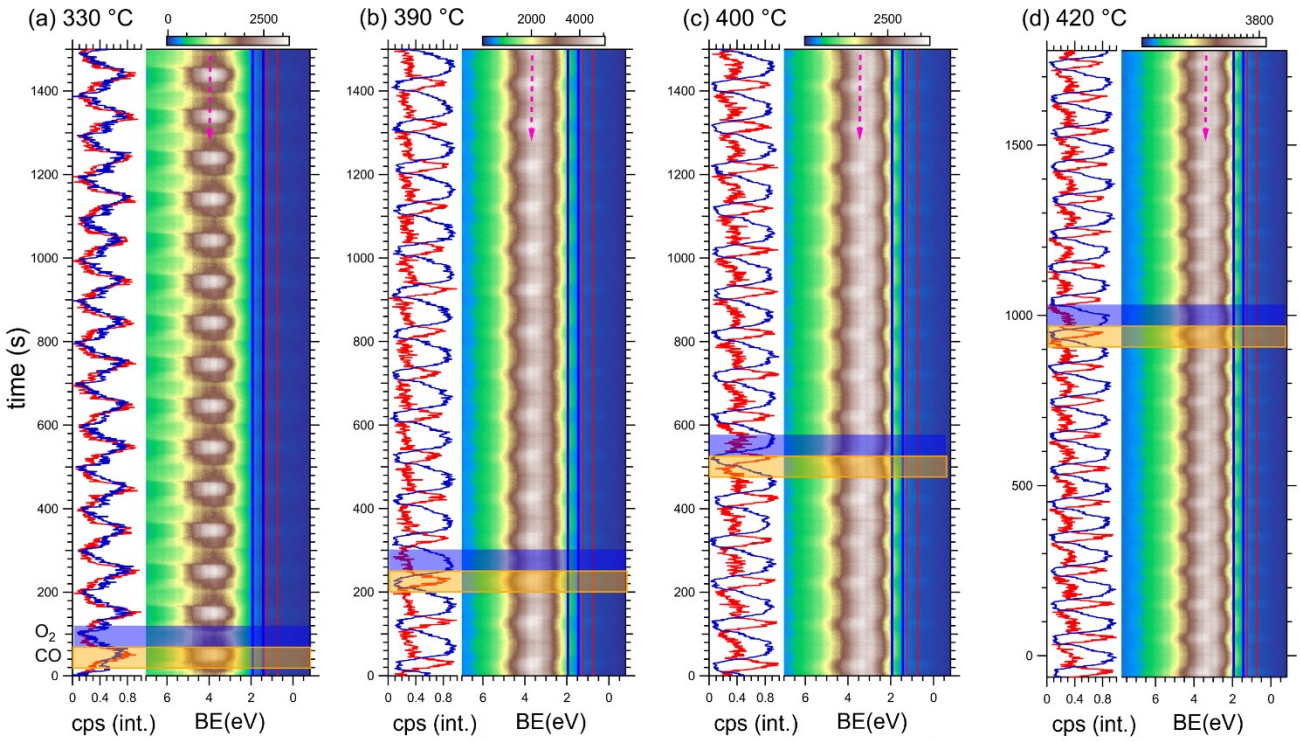

Figure S9: Modulated chemical excitation RPES spectra measured while CO (yellow band) and O_2 (blue band) are pulsed with a mixing flow ratio CO:O_2 = 1. The experiments were performed while ceria is kept at (a) 330 °C, (b) 360 °C, (c) 390 °C and (d) 420 °C, respectively. The pulse duration of each reactant was 40 s. RPES were obtained at the threshold energy corresponding to 124.5 eV and Ce^{4+} excitation. Two vertical profiles are centered on the Ce 4f state at ≈ 1 eV (red) and 1.7 eV (blue). The left panels show the CPS oscillations of both profiles, highlighting the switch between Ce^{3+} and Ce^{4+} species during CO and O_2 injection.

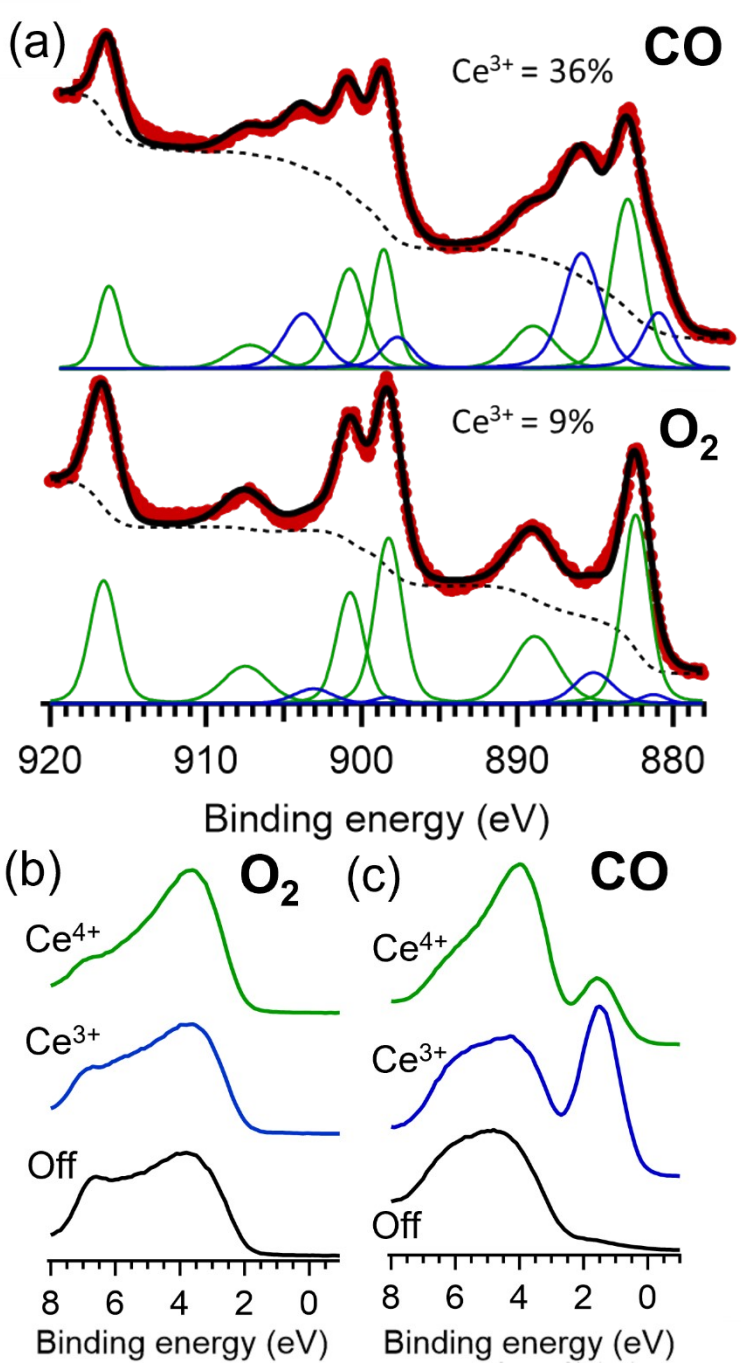

Figure S10: Ce 3d core level spectra obtained during O_2 and CO steady-state conditions at 300 °C (a). The corresponding valence band in off-resonance (115 eV), Ce^{3+} (121.2 eV), and Ce^{4+} (124.5 eV) are shown (b and c).

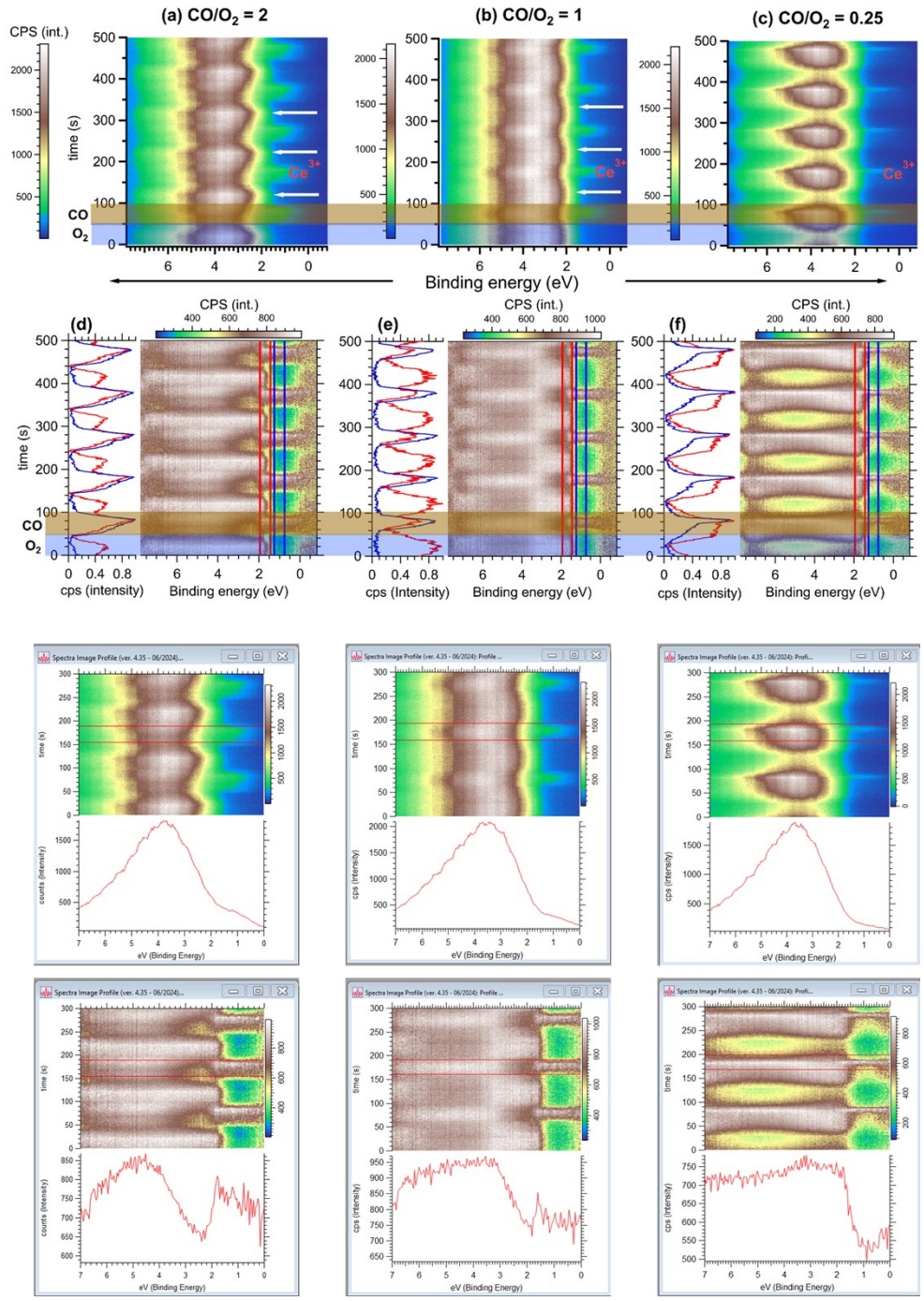

Figure S11: Normalization method: the horizontal profiles (red) on top images are used to normalize the figure. Each profile's maximum is identified and used to divide the entire profile by

this value. This maxima normalization allows the equalization of the data in one direction. This procedure was applied to top images corresponding to CO-rich (a), CO:O_2 = 1 (b), and O_2-rich (c) mixing flows while the sample temperature is kept at 420 °C. The resulting profile integration is shown in the panels below each image. The evolution of the intensity (cps) clearly shows the changes in the Ce 4f state (≈1 eV) as a function of the mixing flows ratio. According to this, the Ce 4f state intensity is highest under CO-rich conditions (a) and reaches a minimum in O_2-rich (c).

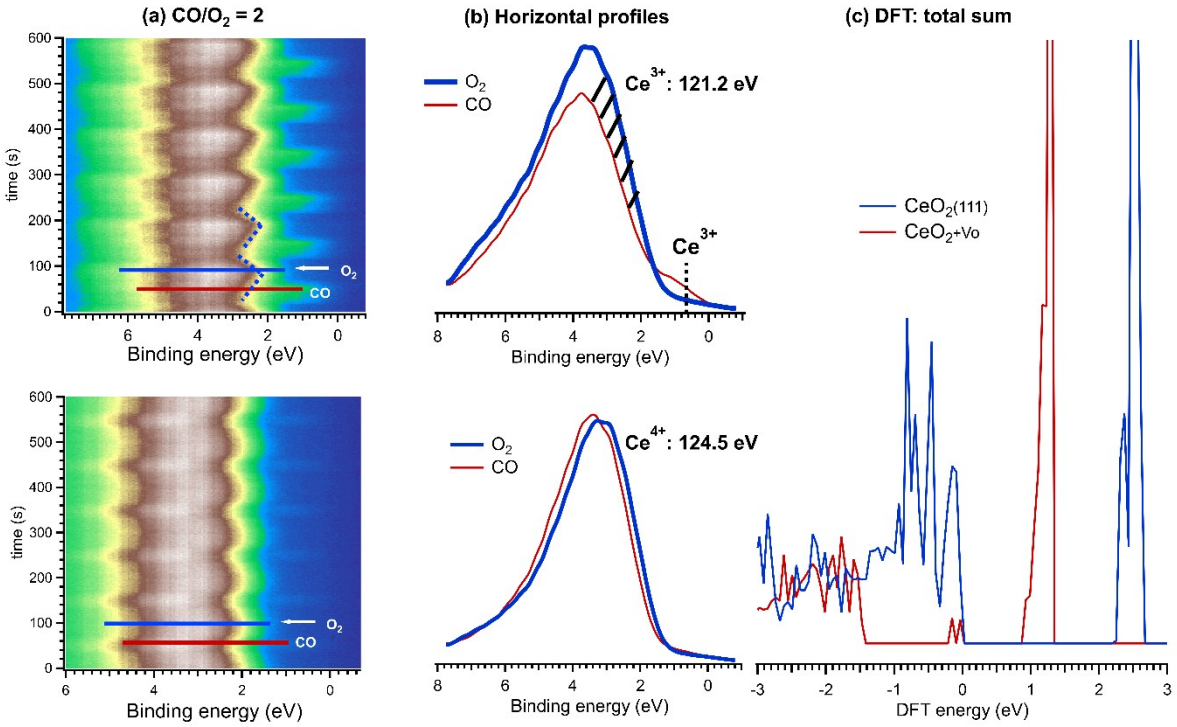

Figure S12: Modulated chemical excitation RPES spectra measured while CO (red line) and O_2 (blue line) are pulsed with a mixing flow ratio CO:O_2 = 2. The experiments were performed while ceria was kept at 420 °C, respectively. The pulse duration of each reactant gas was 40 s. (a) RPES spectra were obtained at the threshold energies corresponding to 121.2 eV (Ce^{3+}) at the top of the figure and 124.5 eV (Ce^{4+}) at the bottom. A "V-shaped" electron density feature (dashed blue line) appears prominently at the Ce^{3+} threshold (121.2 eV). (b) Time-constant spectral profiles extracted from RPES, where the blue profile was obtained under O_2 pulses while the red one was obtained during CO injection, respectively. (c) DFT calculations show the total DOS of CeO_2(111) in blue and CeO_2(111)+V_0 in red, simulating both surface states.

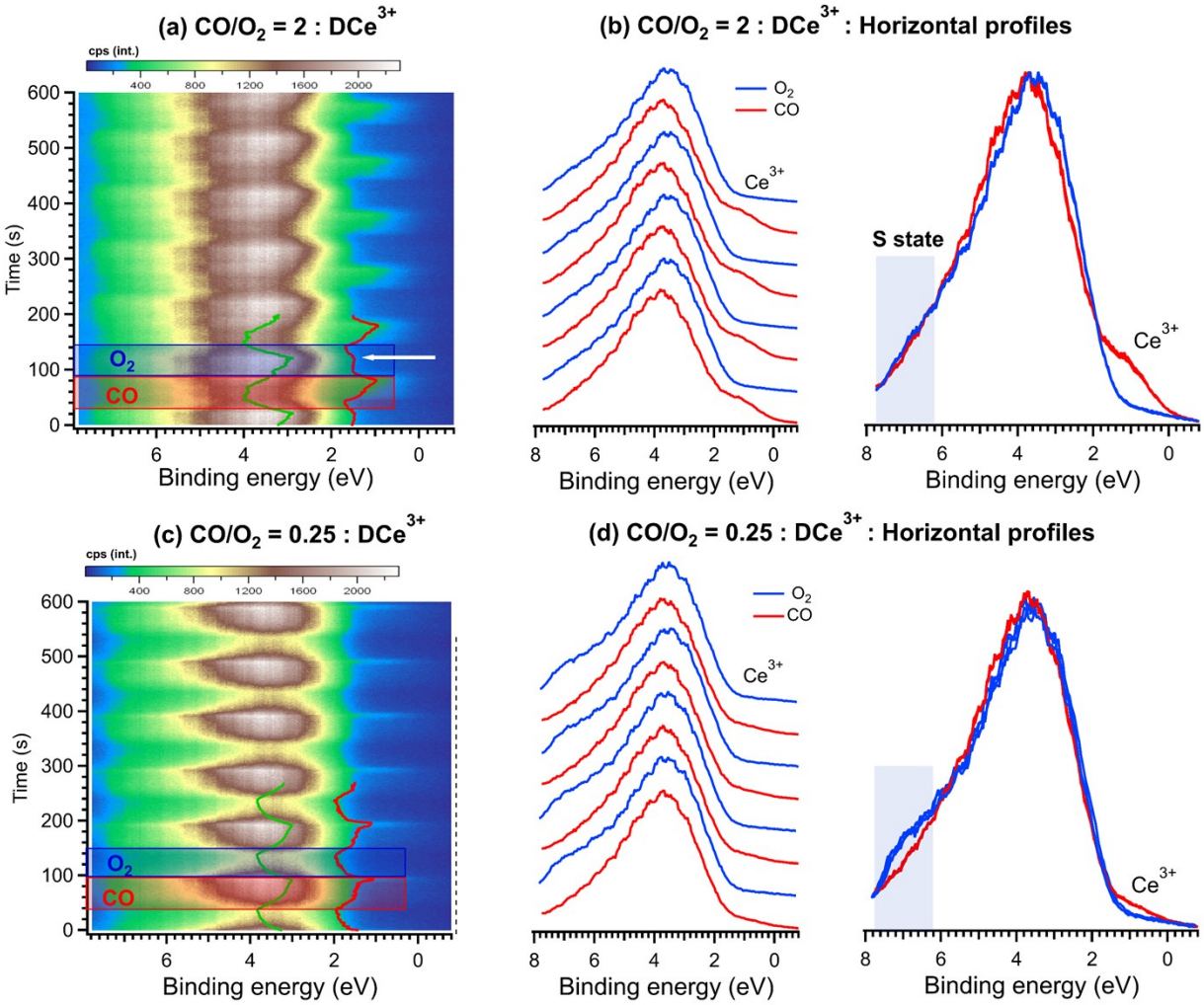

Figure S13: Modulated chemical excitation RPES on CeO_2 under transient conditions of CO and O_2 with the sample kept at 420 °C. (a) Ratio CO:O_2=2. (c) Ratio CO:O_2 =0.25. The pulse duration of each CO and O_2 injection was 40 s/pulse. RPES spectra were obtained at the threshold energy of 121.2 eV (Ce^{3+}). Two vertical profiles are centered at ≈1.2 eV (red) and ≈4 eV (green). The white arrow indicates the persistence of Ce^{3+} state during O_2 injection. On the right (b) and (d) show the horizontal profiles of CO:O_2=2 and CO:O_2=0.25, where the blue profile was obtained under O_2 pulses while the red one was obtained during CO injection, respectively. The blue bar S-state represents the OH groups under O_2 pulses.

Table S1: The energy positions and atomic concentrations of oxygen species are reported here. These values correspond to Figure 3(a) in the NAP-XPS O 1s spectra. The O 1s core level was measured using a photon energy of 590 eV while CeO_2 was exposed to pure O_2 gas flow at a pressure of 0.5 mbar of O_2. The sample temperature was kept constant at 330 °C, 360 °C, 390 °C, 400 °C and 420 °C, respectively. The O 1s show contributions attributed to lattice oxygen (529.5 eV)[2], hydroxyl (531.0 eV)[3,4], peroxide-like oxygen groups (532.7 eV)[5], and O_2 gas phase (gray band)[6,7]. The fitting procedure was carried out using a Voigt function with 30% G/L, using a gwid approx. to 1.4 eV for ceria lattice oxygen, 1.85 eV for hydroxyls, and 2.1 eV for peroxide-like oxygen groups.

Temperature (°C)	Oxygen species	Concentration of species. (at.%)	Energy position (eV)
330 °C	Latt. Oxygen	26	529.5
	OH's	42	530.8
	Peroxide	32	532.7
360 °C	Latt. Oxygen	41	529.6
	OH's	42	530.6
	Peroxide	17	532.8
390 °C	Latt. Oxygen	65	529.5
	OH's	25	530.9
	Peroxide	10	532.5
400 °C	Latt. Oxygen	63	529.5
	OH's	37	531.0
	Peroxide	-	-
420 °C	Latt. Oxygen	64	529.5
	OH's	36	531.0
	Peroxide	-	-

Table S2: Geometric parameters for the Stable Configurations of O_2 and OH species on the partially reduced CeO_2 (111) surface, along with Bader charge (Q), the magnetic moment of Ce^{3+} (m), and energy gap (E_g).

Structure	d_{O-H}(Å)	d_{O-O}(Å)	d_{Ce-O}(Å)	Q^{Ce3+} (e)	Q^{Ce4+} (e)	$m^{Ce3+}(\mu_B)$	E_g (eV)
(a) CeO_2 (111)				-	2.48	-	2.25
(b) CeO_2 (111)+Vo				2.12	2.44	0 .95	0.89:spin up 2.29:spin down
© CeO_2 (111)+Vo+				2.15	2.39	0.94	0.51:spin up 0.32:spin down
(d) CeO_2 (111)+Vo++				2.14	2.48	0.93	0.58 :spin up 1.83:spin down
(e) Superoxo		1.26	2.39	2.12	2.50	0.95	1.45:spin up 2.33:spin down
(f) Peroxo		1.45	2.44	-	2.42	-	1.87
(g) OH-Bridge	0.98		2.50	2.13	2.26	0.95	2.34
(h) OH-Top	0.98		2.49		2.33		1.72

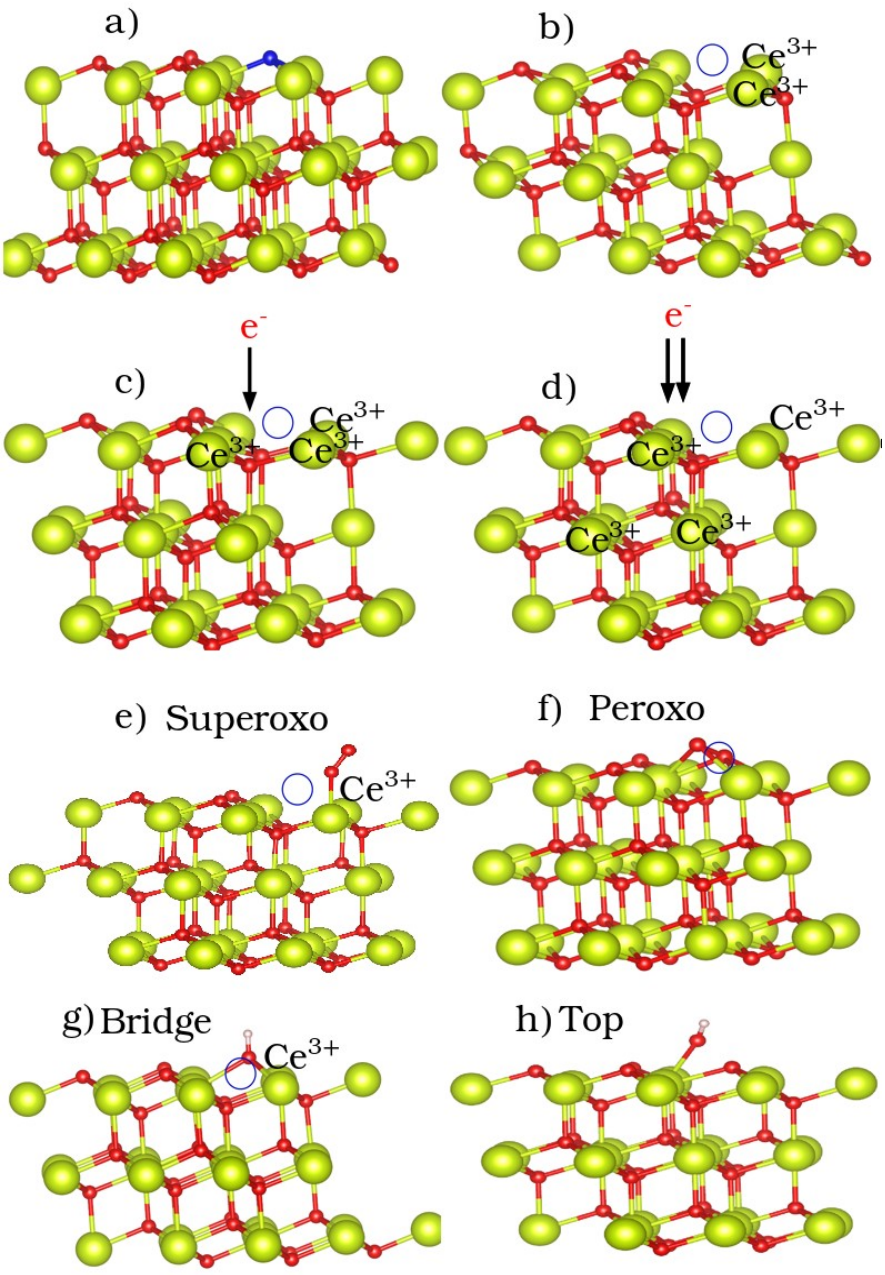

Figure S14: Side views of the optimized atomic structures with (a) stoichiometric CeO_2 (111), (b) an oxygen vacancy, an oxygen vacancy filled with (c) one and (d) two electrons, (e) superoxo, (f) peroxo, (g) bridge OH, and (h) top OH oxygen species adsorbed near the vacancy site. The blue circle highlights an oxygen vacancy within the structure.

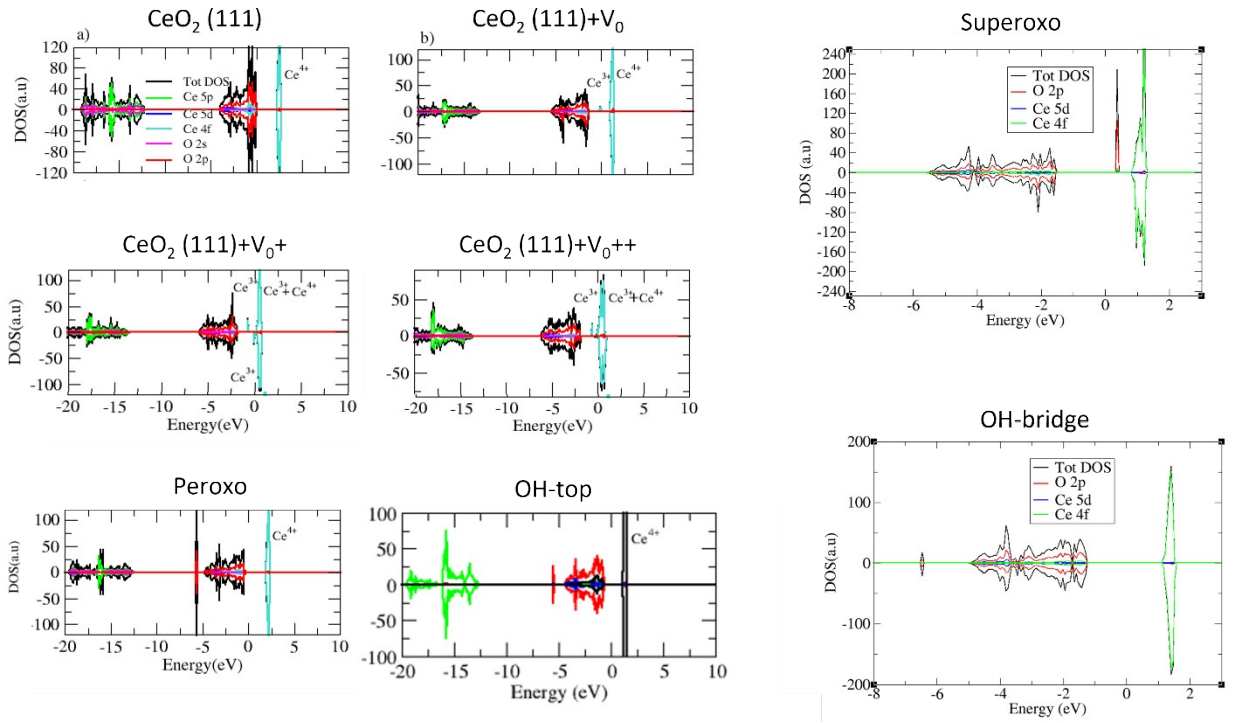

Figure S15: Spin-polarized projected density of states (PDOS) of the different CeO_2(111) optimized conformations presented in Figure S12. The Fermi level is set at 0 eV.

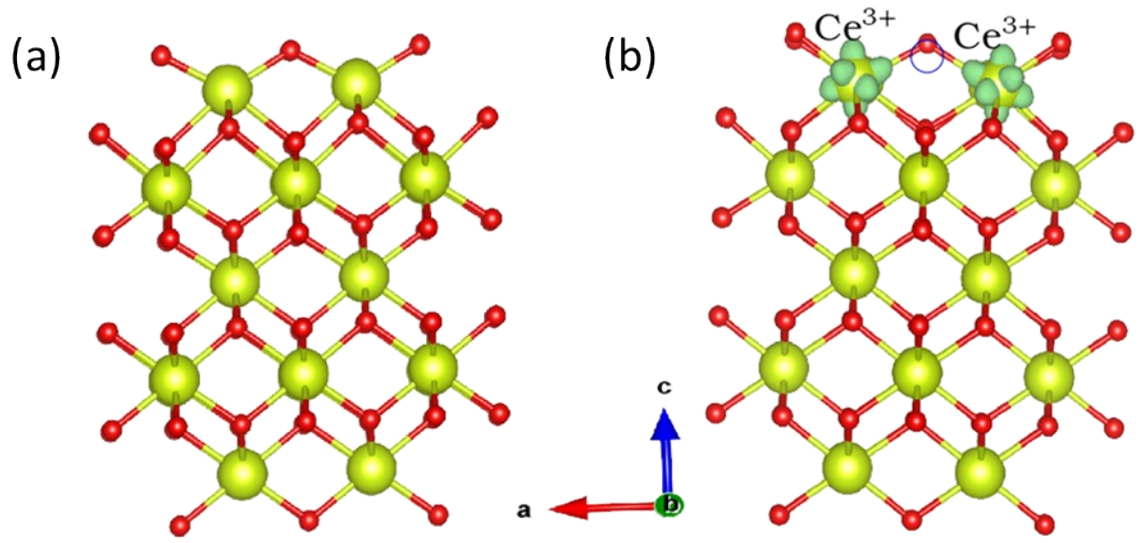

Figure S16: Crystal structure of cerium dioxide (100) surface (a). Calculated charge density (spin difference) of the cerium dioxide (100) surface with an oxygen vacancy (V_0) (b). Green clouds highlight the localized charge on Ce^{3+} ions adjacent to the vacancy. We find that the removal of an oxygen vacancy from this (100) surface is accompanied by the reduction of two adjacent Ce^{4+} ions to Ce^{3+}, a process analogous to that observed on the (111) surface.

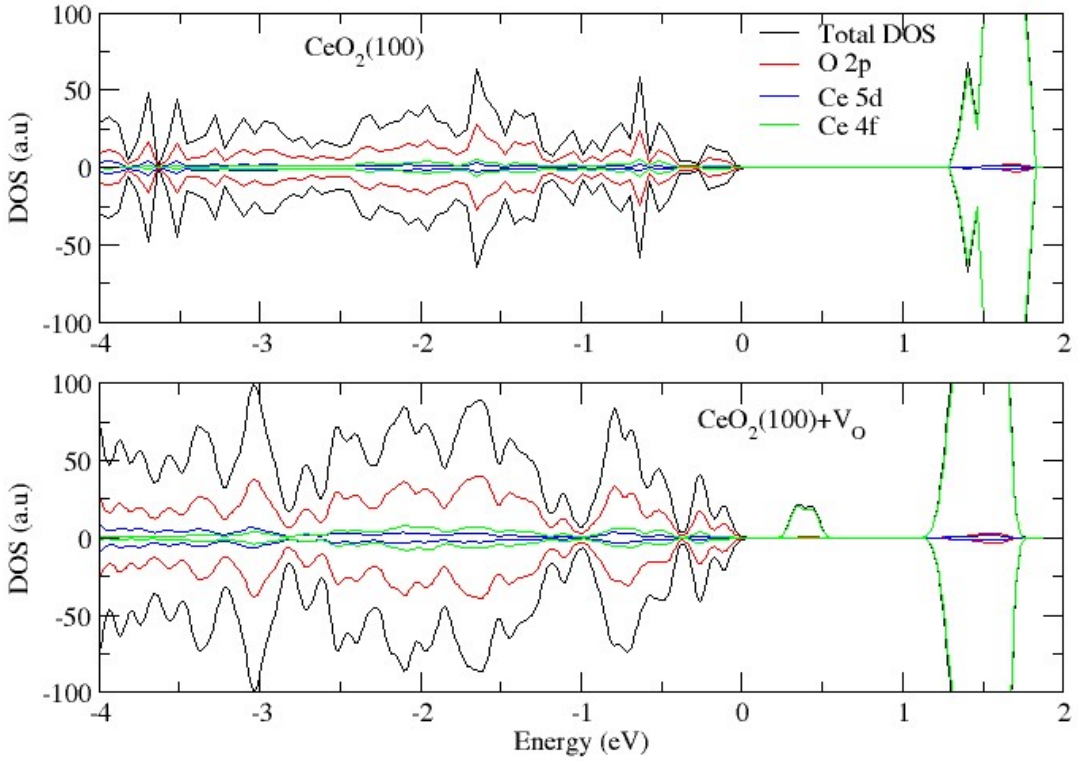

Figure S17: Spin-polarized density of states (DOS) of the optimized structures $CeO_2(100)$ and $CeO2(100)+V_o$. The Fermi level is set at 0 eV.

References

(1)Loridant, S. Raman Spectroscopy as a Powerful Tool to Characterize Ceria-Based Catalysts. *Catal. Today* **2021**, *373*, 98–111. https://doi.org/10.1016/j.cattod.2020.03.044.

(2)Morgan, D. J. Photoelectron Spectroscopy of Ceria: Reduction, Quantification and the Myth of the Vacancy Peak in XPS Analysis. *Surf. Interface Anal.* **2023**, *55* (11), 845–850. https://doi.org/10.1002/sia.7254.

(3)Lykhach, Y.; Johánek, V.; Aleksandrov, H. A.; Kozlov, S. M.; Happel, M.; Skála, T.; Petkov, P. St.; Tsud, N.; Vayssilov, G. N.; Prince, K. C.; et al. Water Chemistry on Model Ceria and Pt/Ceria Catalysts. *J. Phys. Chem. C* **2012**, *116* (22), 12103–12113. https://doi.org/10.1021/jp302229x.

(4)Matolín, V.; Matolínová, I.; Dvořák, F.; Johánek, V.; Mysliveček, J.; Prince, K. C.; Skála, T.; Stetsovych, O.; Tsud, N.; Václavů, M.; et al. Water Interaction with CeO2(1 1 1)/Cu(1 1 1) Model Catalyst Surface. *Catal. Today* **2012**, *181* (1), 124–132. https://doi.org/10.1016/j.cattod.2011.05.032.

(5)Stadnichenko, A. I.; Muravev, V. V.; Koscheev, S. V.; Zaikovskii, V. I.; Aleksandrov, H. A.; Neyman, K. M.; Boronin, A. I. Study of Active Surface Centers of Pt/CeO_2 Catalysts Prepared Using Radio-Frequency Plasma Sputtering Technique. *Surf. Sci.* **2019**, *679*, 273–283. https://doi.org/10.1016/j.susc.2018.10.002.

(6)Avval, T. G.; Chatterjee, S.; Hodges, G. T.; Bahr, S.; Dietrich, P.; Meyer, M.; Thißen, A.; Linford, M. R. Oxygen Gas, O_2(g), by near-Ambient Pressure XPS. *Surf. Sci. Spectra* **2019**, *26* (1), 014021. https://doi.org/10.1116/1.5100962.

(7)Blomberg, S.; Hoffmann, M. J.; Gustafson, J.; Martin, N. M.; Fernandes, V. R.; Borg, A.; Liu, Z.; Chang, R.; Matera, S.; Reuter, K.; et al. *In Situ* X-Ray Photoelectron Spectroscopy of Model Catalysts: At the Edge of the Gap. *Phys. Rev. Lett.* **2013**, *110* (11), 117601. https://doi.org/10.1103/PhysRevLett.110.117601.